Food Chemistry 230 (2017) 627–636

Contents lists available at ScienceDirect

Food Chemistry

journal homepage: www.elsevier.com/locate/foodchem

Contributions of molecular size, charge distribution, and specific amino acids to the iron-binding capacity of sea cucumber (*Stichopus japonicus*) ovum hydrolysates

Na Sun, Pengbo Cui, Ziqi Jin, Haitao Wu, Yixing Wang, Songyi Lin *

School of Food Science and Technology, Dalian Polytechnic University, National Engineering Research Center of Seafood, Dalian 116034, PR China

ARTICLE INFO

Article history:
Received 13 December 2016
Received in revised form 27 February 2017
Accepted 13 March 2017
Available online 14 March 2017

Keywords:
Sea cucumber ovum
Iron binding
Molecular size
Amino acids
Characterization

ABSTRACT

This study investigated the contributions of molecular size, charge distribution and specific amino acids to the iron-binding capacity of sea cucumber (*Stichopus japonicus*) ovum hydrolysates (SCOHs), and further explored their iron-binding sites. It was demonstrated that enzyme type and degree of hydrolysis (DH) significantly influenced the iron-binding capacity of the SCOHs. The SCOHs produced by alcalase at a DH of 25.9% possessed the highest iron-binding capacity at 92.1%. As the hydrolysis time increased, the molecular size of the SCOHs decreased, the negative charges increased, and the hydrophilic amino acids were exposed to the surface, facilitating iron binding. Furthermore, the Fourier transform infrared spectra, combined with amino acid composition analysis, revealed that iron bound to the SCOHs primarily through interactions with carboxyl oxygen of Asp, guanidine nitrogen of Arg or nitrogen atoms in imidazole group of His. The formed SCOHs-iron complexes exhibited a fold and crystal structure with spherical particles.

1. Introduction

Iron is an essential microelement that constitutes the spatial structure of hemoglobin, cytochromes, and enzymes, and is involved in a wide variety of biological functions, including respiration, energy metabolism regulation and cell proliferation (Puig, Askeland, & Thiele, 2005). However, iron deficiency affects more than two billion people worldwide and remains the top cause of anemia (McLean, Cogswell, Egli, Wojdyla, & De Benoist, 2009). The reported prevalence of iron deficiency in the absence of dietary fortification is approximately 40% in preschool children, 30% in menstruating girls and women, and 38% in pregnant women (Stevens et al., 2013). These rates reflect the increased physiological need for dietary iron during specific life stages and according to sex (Camaschella, 2015).

Dietary iron is available mainly in two forms: heme and non-heme iron. Heme iron, which only comes from haemoglobin and myoglobin in animal-based food, can be absorbed in the duodenum with a 15–35% absorption rate (Pereira & Vicente, 2013). The absorption rate of dietary non-heme iron is only below 10% (Martınez-Navarrete, Camacho, Martınez-Lahuerta, Martınez-Monzó, & Fito, 2002). The poor absorption of non-heme iron is attributed to its poor solubility at near-neutral pH and its interactions with food components, mainly phytic acid, polyphenols, and fibres (Hurrell & Egli, 2010). It is known that some dietary compounds, such as certain amino acids (His, Glu, Asp, and Cys) and peptides released during proteolytic digestion enhance iron absorption (Storcksdieck, Bonsmann, & Hurrell, 2007). These compounds may bind with iron, forming soluble complexes and thus improving iron absorption.

Various studies have revealed the beneficial effect on iron binding by peptides produced via enzymatic hydrolysis of various proteins, such as casein, whey protein, muscle protein and soy protein (O'Loughlin, Kelly, Murray, FitzGerald, & Brodkorb, 2015; Storcksdieck et al., 2007; Wang, Li et al., 2011; Wu, Liu, Zhao, & Zeng, 2012; Zhang, Huang, & Jiang, 2014). Enzymatic hydrolysis is a commonly used method for producing bioactive peptides (Sun et al., 2016). However, the choice of proteolytic enzyme seems to be crucial to the iron-binding capacity, because its speci-

Abbreviations: SCO, sea cucumber ova; SCOHs, sea cucumber ovum hydrolysates; DH, degree of hydrolysis; HPLC, High Performance Liquid Chromatography; UV–Vis, UV–visible; FTIR, Fourier transform infrared spectroscopy; Asp, aspartic acid; Arg, arginine; His, histidine.

* Corresponding author at: School of Food Science and Technology, Dalian Polytechnic University, National Engineering Research Center of Seafood, Ministry of Science and Technology, No. 1 Qinggongyuan, Ganjingzi District, Dalian 116034, PR China.

E-mail address: linsongyi730@163.com (S. Lin).

http://dx.doi.org/10.1016/j.foodchem.2017.03.077
0308-8146/

fic action will influence the final composition of the hydrolysis products, mainly the average peptide length and exposure of the side chains (Adler-Nissen, 1986). Therefore, it is known that enzyme type and degree of hydrolysis will significantly influence the iron-binding capacity of the hydrolysates (Wang, Li et al., 2011; Zhang et al., 2014; Zhou et al., 2012). However, the change in peptide size, charge distribution, and polar groups during the process of hydrolysis, as well as their relationships with the iron-binding capacity of the hydrolysates, remain to be clarified. Regarding the iron-binding sites of peptides, studies with iron-peptide complexes have revealed that the major iron-binding sites correspond primarily to the carboxyl groups of Asp and Glu (Huang, Ren, & Jiang, 2011; O'Loughlin et al., 2015). Sulphydryl groups and nitrogen-rich groups, such as the amino group of Lys, imidazole of His, and guanidine of Arg may also be involved in iron binding (Nicholson et al., 1997; Torres-Fuentes, Alaiz, & Vioque, 2012).

Sea cucumber (*Stichopus japonicus*) is one of the most important holothurian species in coastal fisheries. The aquaculture of sea cucumber has increased rapidly in Asia in recent decades (Anderson, Flemming, Watson, & Lotze, 2011). The total output of sea cucumber has exceeded 200,000 tons in China (China Fishery Statistical Yearbook, 2015). Sea cucumber ova are deemed as low-value by-products generated during industrial processing, and remain to be fully utilized as value-added materials. In our previous work, we found that defatted sea cucumber ova are rich in protein (80.9 ± 2.2% protein content) and that the relative Asp and Glu contents could reach 23% (unpublished data). It is speculated that sea cucumber ova may be a good source of metal-binding peptides. Hence, the aim of this study was to produce iron-binding peptides from sea cucumber ova though enzymatic hydrolysis and to investigate the dynamic variations in molecular size, charge distribution, and exposure of specific amino acids during the hydrolysis process to clarify their contributions to the iron-binding capacity of the hydrolysates. Further, the structural and physical characteristics of complexes of sea cucumber ovum hydrolysates and iron were investigated. This may aid immensely in the understanding of the nature of iron-binding peptides and associated iron binding mechanisms.

2. Materials and methods

2.1. Materials

Sea cucumber ova (SCO) were obtained from the Shangpintang Marine Biology Co., Ltd. (Dalian, China). Alcalase 2.4 L and neutrase 2.4 L were donated by Novozyme (Bagsvaerd, Denmark). Trypsin (from porcine pancreas) was purchased from Bio Basic Inc. (Toronto, Canada). Papain (a cysteine protease from papaya latex) and flavourzyme were obtained from Sangon Biotech Co. Ltd (Shanghai, China) and Pangbo Biological Engineering Co. Ltd (Nanning, Guangxi, China), respectively. All other chemicals and reagents used in this study were of analytical grade and commercially available.

2.2. Generation of sea cucumber ovum hydrolysates (SCOHs)

Sea cucumber ova were defatted with hexane/ethanol (3:1 v/v) at 50 °C for 6 h, filtered and naturally air-dried at room temperature. The defatted sea cucumber ova (SCO) powder was mixed with Milli-Q (Millipore, Bedford, MA) water at a ratio of 1:50 (w/v). The mixture was heated in boiling water for 10 min, and then hydrolyzed with trypsin (37 °C, pH 8.0), alcalase (50 °C, pH 8.5), neutrase (50 °C, pH 7.0), papain (50 °C, pH 7.0), or flavourzyme (37 °C, pH 8.0) at a dose of 3000 U/g protein. After 3 h of hydrolysis, the enzyme was inactivated by heating at 95 °C for 10 min. The suspension was centrifuged at 12,000*g* for 20 min at 4 °C and the precipitate was discarded. The supernatant was freeze-dried and stored at −20 °C for later investigation.

2.3. Determination of degree of hydrolysis

The determination of degree of hydrolysis (DH), defined as the ratio of the number of peptide bonds cleaved (h) to the total number of peptide bonds in a protein substrate (h_{tot}), was carried out using the pH-stat method (Adler-Nissen, 1986). The formula for the calculation was as follows:

$$DH = \frac{h}{h_{tot}} \times 100\% = B \times N_b \times \frac{1}{\alpha} \times \frac{1}{MP} \times \frac{1}{h_{tot}} \times 100\% \quad (1)$$

B is the volume (ml) of NaOH consumed to keep the pH constant during the enzymatic reaction, N_b is the normality of NaOH, MP is the mass of the protein (g), and h_{tot} is the total number of peptide bonds in the substrate (mmol/g protein). α is the average degree of dissociation of the α-NH_2 groups released during hydrolysis and was calculated as follows:

$$\alpha = \frac{10^{pH-pK}}{1 + 10^{pH-pK}} \quad (2)$$

The values of pH and pK were the values at which the proteolysis was conducted.

2.4. Iron-binding capacity assay

Iron-binding capacity was determined by measuring the formation of the Fe^{2+}-ferrozine complex according to the method of O'Loughlin et al. (2015). At room temperature, 1 mg/ml samples (1 ml) were mixed with 1.35 ml of Milli-Q water and 50 μl of 2 mM $FeCl_2$ for 10 min. After the reaction, 100 μl of 5 mM ferrozine was added and gently mixed for 10 min. The absorbance at 562 nm was determined using a microplate reader (Tecan Infinite 200 PRO, Männedorf, Switzerland). The experiment was performed in triplicate and values are expressed as mean ± standard deviation (SD).

2.5. Preparation of sea cucumber ovum hydrolysates-iron complexes

Lyophilized SCOHs were dissolved in Milli-Q water at a concentration of 30 mg/ml, and $FeCl_2{\cdot}4H_2O$ was subsequently added to be a final concentration of 50 mM. The reaction was carried out in a shaker at 25 °C and pH 7.0 for 30 min, and then ethanol was added to the reactant to a final concentration of 85% to remove free iron. After centrifugation at 12,000*g* for 5 min, the precipitate was collected, freeze-dried, and labelled as SCOHs-iron.

2.6. Determination of molecular weight distribution

The molecular weight (MW) distribution profiles of the SCOHs treated with alcalase for different hydrolysis times were determined using gel-permeation chromatography on a Superdex Peptide 10/300 GL column (300 × 10 mm, GE Healthcare Co., Little Chalfont, Buckinghamshire, UK) with an Elite P230 high-performance liquid chromatography (HPLC) system (Elite Analytical Instruments Co., Ltd., Dalian, China) according to the method of Wu et al. (2016) with some modifications. Ten microlitres of SCOH solution (2 mg/ml, filtered through 0.45 μm filter) were loaded onto the HPLC (mobile phase: acetonitrile/water/trifluoroacetic acid = 30:70:0.1 v/v/v). The sample was eluted at a flow rate of 0.4 ml/min and monitored at 220 nm by an ultraviolet (UV) detector. The standards used were cytochrome *c* (12,500 Da), aprotinin (6512 Da), β-amyloid (4514 Da), vitamin B_{12} (1355 Da), MOG

(2582 Da), GSH (307 Da) and glycine (75 Da). The standards yielded a linear retention time (x) versus log MW (y) regression curve in the MW range of 75–12,500 Da: $y = -0.0713x + 5.6943$ ($R^2 = 0.9906$). The HPLC chromatograph was divided into six parts according to the retention time. The molecular weight ranges of the six parts were >5000, 5000–3000, 3000–1000, 1000–500, 500–200, and < 200 Da, providing the profile of different molecular weight peptides and individual amino acids. The percentage content for each fraction is represented by its percentage area under the curve.

2.7. Zeta potential measurement

The zeta potential of the SCOHs treated with alcalase for different hydrolysis times was determined using a Zetasizer Nano ZS90 particle size analyzer (Malvern Instruments Ltd., Malvern, UK). The measurement was performed according to the method from the previous studies of Lin et al. (2017). A test sample was mixed for 5 s, and then transferred to a Malvern polystyrene U-shaped cell. Subsequently, the cell temperature was stabilized at 25 °C for 5 s, and each of the measurements was conducted at 25 °C and repeated 12 times.

2.8. Amino acid composition analysis

The amino acid profiles of SCOHs-iron were determined using HPLC coupled with a ODS amino acid column (4.6 mm × 250 mm), Elite-AAK (Elite Analytical Instruments Co., Ltd., Dalian, China), according to the method in our previous report (Wu et al., 2016). All amino acid residues were determined after hydrolysis at 110 °C for 24 h with 6 M HCl prior to derivatization with 2,4-dinitrofluorobenzene. The concentrations of specific amino acids were determined from their respective absorption intensities, which were calibrated to the known concentrations of amino acid standards (Elite, Dalian, China). Alkaline hydrolysis was conducted for the determination of tryptophan levels.

2.9. Structural characterization of sea cucumber ovum hydrolysates-iron complexes

2.9.1. Ultraviolet–visible spectroscopy

The freeze-dried SCOHs and SCOHs-iron were dissolved in Milli-Q water at a concentration of 0.1 mg/ml, respectively. The UV–visible (UV–Vis) spectra of SCOHs and SCOHs-iron were recorded over the wavelength range from 190 to 800 nm by a UV–Vis spectrophotometer (Perkin Elmer, Salem, MA).

2.9.2. Fourier transform infrared spectroscopy (FTIR) measurement

One milligram of freeze-dried SCOHs or SCOHs-iron was mixed with 100 mg of dry KBr. The mixture was ground into a fine powder and compressed into a thin disc. All FTIR spectra were recorded by a FT-IR spectrometer (Perkin Elmer, Salem, MA) over a wavenumber region between 4000 and 400 cm^{-1} at a resolution of 4 cm^{-1}. All measurements were performed in a dry atmosphere at room temperature (25 ± 1 °C). The peak signals in the spectra were analyzed using OMNIC 8.2 software (Thermo Nicolet Co., Madison, WI, USA).

2.10. Microstructure analysis of SCOHs-iron complexes

The microstructure of SCOHs and SCOHs-iron was performed by a scanning electron microscope (JSM-7800F, JEOL Ltd., Tokyo, Japan) according to the method of Jin et al. (2017) with some modifications. 1 mg of freeze-dried SCOHs and SCOHs-iron was placed on an adhesive tape attached to a circular aluminum specimen stub and coated with gold-palladium for 90 s under 15 mA current. The specimens were observed at an acceleration voltage of 5 kV.

2.11. Statistical analysis

All experiments were performed in triplicate. All data were subjected to a one-way ANOVA using SPSS software (SPSS 18.0, SPSS Inc., Chicago, IL). Comparison of means was performed with a LSD test, with the confidence level set at $P < 0.05$. Correlation coefficients were determined using the Spearman rank method by SPSS software. Spearman r-values and the associated *P*-values are shown in the relevant figures.

3. Results and discussion

3.1. Effect of proteases on degree of hydrolysis and iron-binding capacity of SCOHs

The DHs and iron-binding capacities of SCOHs prepared using five commercially available enzymes (trypsin, alcalase, neutrase, papain, and flavourzyme) were measured. Hydrolysates produced with alcalase showed the best DH, which was significantly higher than those of hydrolysates produced with trypsin, neutrase, papain, and flavourzyme ($P < 0.05$) (Fig. 1A). The greater hydrolysis of SCO by alcalase may be attributed to its capacity to break large numbers of peptide bonds (Adamson & Reynolds, 1996). Alcalase contains several different proteinases, each with different specificities, because it is a relatively crude bacterial extract of *Bacillus licheniformis* (Sukan & Andrews, 1982). Furthermore, different enzymatic hydrolysates possessed different capacities to bind with iron. Hydrolysates obtained with alcalase exhibited the highest iron-binding capacity at 90.2%, whereas those obtained with flavourzyme showed the lowest ($P < 0.05$) (Fig. 1A). Kim et al. (2007) and Zhou et al. (2012) have shown that alcalase is noticeably effective in producing iron-binding peptides from whey protein and β-lactoglobulin hydrolysates, respectively. Different hydrolytic actions of the enzymes result in different free and total amino acid compositions in the hydrolysate fractions (Caetano-Silva, Bertoldo-Pacheco, Paes-Leme, & Netto, 2015), and free amino acids have lower iron-binding capacities than peptides do (Huang et al., 2011). The endopeptidase activity of alcalase led to a low free amino acid content in the hydrolysate fractions (Smyth & FitzGerald, 1998), whereas the exopeptidase activity of flavourzyme was responsible for the presence of 60% of the free amino groups from free amino acids in the fraction (Nchienzia, Morawicki, & Gadang, 2010).

3.2. Effect of hydrolysis time on iron-binding capacity of SCOHs

The iron-binding capacities of SCOHs obtained after different hydrolysis periods were investigated, and the results are shown in Fig. 1B. The iron-binding capacity increased as the hydrolysis time increased. The hydrolysates with a DH of 25.9%, obtained after a hydrolysis time of 3 h, possessed the highest iron-binding capacity at 92.1%. However, the iron-binding ability decreased if the hydrolysis time exceeded 3 h, which meant that the hydrolysis time had a significant effect on the binding reaction between the SCOHs and iron ions. A similar result was reported by Wang, Zhou, Tong, and Mao (2011), where the Zn-chelating capacity of yak casein hydrolysates increased in parallel with hydrolysis time, reaching a peak at 6 h, and then decreased as hydrolysis time increased. Moreover, a close correlation ($r = 0.96$, $P < 0.01$) was observed between the DH and iron-binding capacity (Fig. 1C). It is worth noting that the ability of proteins or peptides to chelate Fe^{2+} is very important for their antioxidant activity, because

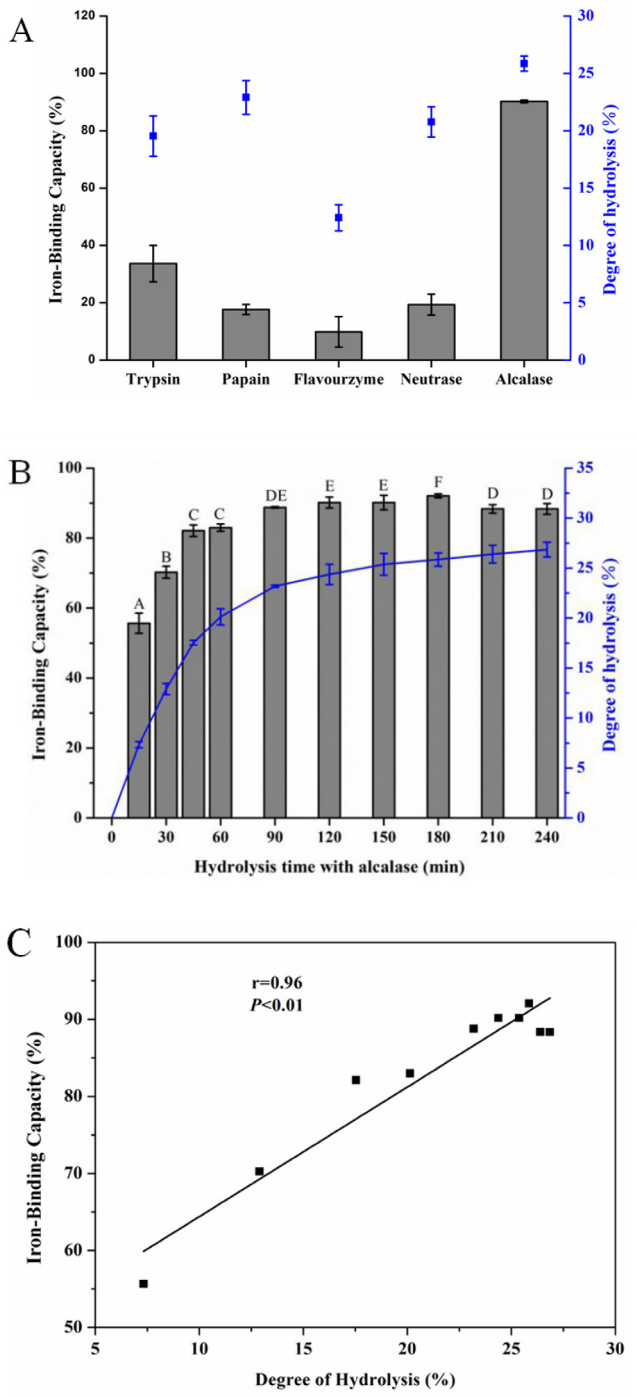

Fig. 1. Effects of enzyme type and degree of hydrolysis on iron-binding capacity of the SCOHs. (A) Effects of enzyme type on iron-binding capacity and degree of hydrolysis of the SCOHs. (B) Effects of different hydrolysis time on iron-binding capacity of the SCOHs prepared by alcalase. (C) Correlation of iron-binding activity of the SCOHs with degree of hydrolysis. The Spearman Rank Correlation Coefficient r-value and the associated *P*-value are shown for each panel.

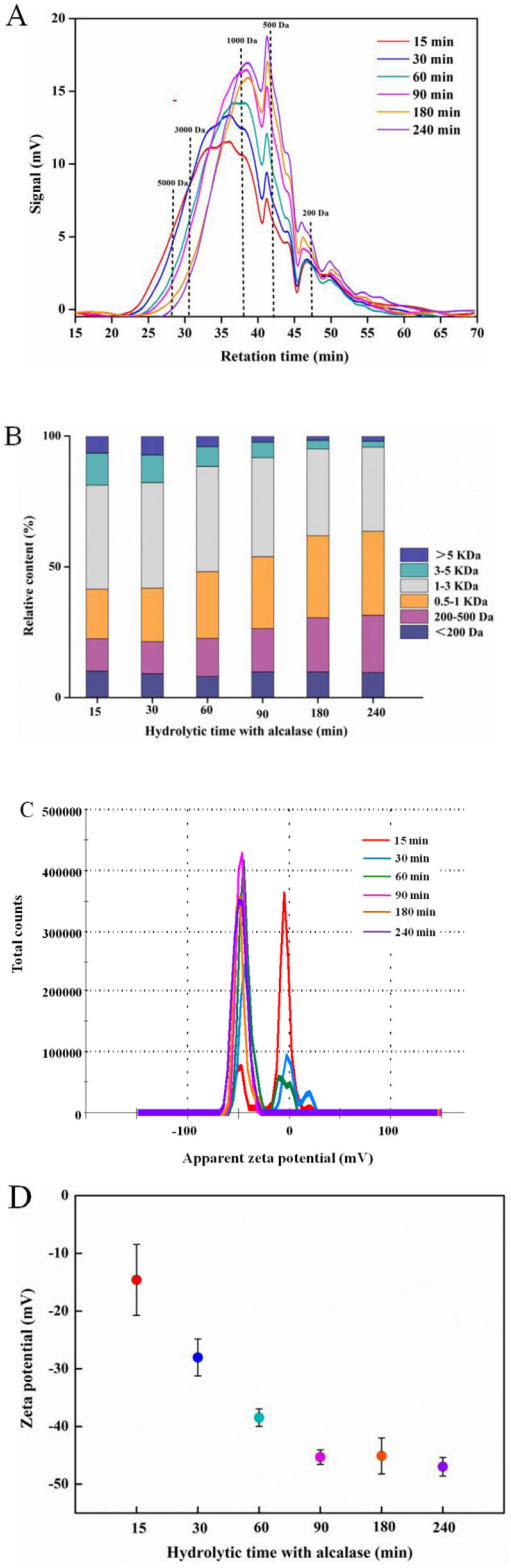

Fig. 2. The molecular weight distribution and zeta potential profile of the SCOHs treated with alcalase at different hydrolysis time. (A) Molecular mass distribution profile of the SCOHs following gel-permeation chromatography on a Superdex Peptide 10/300 GL column with an Elite P230 HPLC system. (B) The relative content of different molecular weight hydrolysates obtained after different hydrolysis time. (C) Zeta potential profile of the SCOHs by a Zetasizer Nano ZS90 particle size analyzer. (D) The zeta potential values of the SCOHs treated with alcalase after different hydrolysis time.

"site-specific, metal-catalyzed oxidation" may occur (Wang & Xiong, 2005). The transition metals iron and copper catalyse the generation of reactive oxygen species, including hydroxyl radical (·OH) and superoxide radical ($O_2^{\cdot-}$), leading to oxidation of unsaturated lipids and promoting oxidative damage at different levels

(Carrasco-Castilla et al., 2012). These results indicate that the degree of enzyme treatment influences the iron-binding activity and antioxidant properties of the SCOHs obtained with alcalase.

3.3. Molecular mass distribution

The relationship between the molecular weight distribution of hydrolysates and their iron-binding properties is not fully understood. To date, both low-molecular-weight and high-molecular-weight peptides have been reported to be able to bind iron to a significant extent. Torres-Fuentes et al. (2012) revealed that low-molecular-weight (below 500 Da) peptides derived from chickpea protein exhibited higher iron-binding activity than the larger peptides (above 500 Da) did. However, Seth and Mahoney (2000) found that iron was mostly bound to large peptides (>10 kDa) generated from chicken muscle protein and only 10% was bound to small peptides or amino acids. To determine the effect of the molecular size of SCOHs on iron-binding activity, the molecular weight distribution of hydrolysates treated with alcalase for different hydrolysis times was determined using an HPLC apparatus equipped with a Superdex Peptide 10/300 GL column (Fig. 2A). The percentage content for each molecular weight range is represented by its percentage area under the curve and reported in Fig. 2B. As the hydrolysis time increased, the relative proportion of fractions between 200 and 1000 Da increased significantly from 21.3% to 54.0% ($P < 0.05$) and, inversely, the proportion of fractions larger than 1000 Da decreased markedly from 58.5% to 36.4% ($P < 0.05$). It is noteworthy that the iron-binding capacity of SCOHs increased significantly from 55.7% to 92.1% as the molecular weight decreased. According to correlation analysis, the proportion of small fractions between 200 and 1000 Da had a positive correlation ($r = 0.88$, $P < 0.05$) with iron-binding activities. On the other hand, there was a negative correlation ($r = 0.94$, $P < 0.01$) between the iron-binding activity and the content of fractions larger than 3000 Da. These results indicate that the molecular mass of SCOHs is an important factor in iron-binding capacity, and that low-molecular-weight hydrolysates are beneficial to iron binding.

3.4. Zeta potential analysis

Zeta potential is an important physicochemical parameter that can reflect the surface charge state of particles in dispersion systems. The partial ionization of various amino acid residues produces the surface charge of protein particles (Vanapalli & Coupland, 2000). Fig. 2 (C and D) presents the zeta potential values of the SCOHs obtained after different hydrolysis times. The negative charges on the SCOHs increased gradually with increased hydrolysis time, although the SCOHs obtained after different hydrolysis times remained negatively charged. Further, a positive correlation ($r = 0.99$, $P < 0.01$) between zeta potential and iron-binding activity was observed with SCOHs obtained after different hydrolysis times. Thus, the hydrolysis leads to the exposure of a growing number of negatively charged moieties, such as carboxyl groups ($-COO^-$), which may be the iron-binding sites.

3.5. Amino acid composition analysis

The amino acid profiles of complexes of iron and SCOHs obtained after different hydrolysis periods were analyzed and are shown in Table 1. The contents of hydrophilic amino acids including aspartic acid (Asp), arginine (Arg) and histidine (His) increased gradually as the hydrolysis time increased (Table 1) and showed a positive correlation with iron-binding activities (Fig. 3A, B and C). In contrast, hydrophobic amino acids including methionine (Met) and valine (Val) decreased with the increase in hydrolysis time (Table 1) and were negatively correlated with iron-binding activities (Fig. 3E and F). O'Loughlin et al. (2015) has reported that ferrous-chelating capability was higher in the more hydrophilic than in the hydrophobic fraction of whey protein isolate hydrolysate. Therefore, it appears that the hydrolysis induces the exposure of hydrophilic amino acids containing Asp, His, and Arg residues, which contribute to the iron-binding activities of the SCOHs.

Aspartic acid has been recognized as an important amino acid that contributes to the iron binding capacity of many peptides. Caetano-Silva et al. (2015) isolated many iron-binding peptides from whey protein hydrolysates and subsequently analyzed the sequences of these isolated peptides using liquid chromatography-tandem mass spectrometry. More than 80% of the sequences identified showed the presence of Asp, and all of them had from 2 to 5 Asp residues, which suggests that the Asp residue may have high affinity for iron. Furthermore, Lee and Song (2009) and Wu et al. (2012) also found high levels of Asp in the sequences of peptides from porcine blood plasma protein and anchovy muscle protein, respectively, and the Asp residue was

Table 1
Amino acid composition of SCOHs-iron complexes obtained after different hydrolysis time.

Amino acids	Hydrolysis time					
	15 min	30 min	60 min	90 min	180 min	240 min
Asp	13.23 ± 0.12^{a}	14.13 ± 1.30^{ab}	14.55 ± 0.27^{b}	14.55 ± 0.43^{b}	14.81 ± 0.19^{b}	14.94 ± 0.37^{b}
Glu	16.42 ± 0.31^{a}	17.78 ± 1.81^{ab}	18.37 ± 0.59^{b}	17.71 ± 0.51^{b}	17.77 ± 0.25^{b}	18.46 ± 0.73^{b}
Ser	3.55 ± 0.01^{a}	3.42 ± 0.18^{ab}	3.83 ± 0.48^{a}	2.85 ± 1.34^{ab}	2.32 ± 0.04^{b}	2.95 ± 0.57^{ab}
Arg	3.57 ± 0.28^{a}	3.56 ± 0.33^{a}	3.80 ± 0.18^{a}	4.88 ± 0.51^{b}	5.29 ± 0.09^{b}	4.82 ± 1.02^{b}
Gly	8.09 ± 0.24^{a}	8.50 ± 0.79^{ab}	7.70 ± 0.13^{ac}	7.83 ± 0.24^{a}	7.43 ± 0.07^{ac}	7.78 ± 0.39^{ac}
Thr	4.15 ± 0.06^{a}	4.17 ± 0.38^{a}	3.99 ± 0.17^{ab}	4.02 ± 0.23^{ab}	3.64 ± 0.33^{b}	4.51 ± 0.28^{ac}
Pro	3.17 ± 0.09^{a}	3.11 ± 0.11^{a}	3.13 ± 0.07^{a}	3.04 ± 0.13^{ab}	3.17 ± 0.05^{a}	3.24 ± 0.17^{ac}
Ala	3.98 ± 0.05^{ab}	4.13 ± 0.31^{ab}	4.00 ± 0.14^{ab}	3.77 ± 0.11^{abc}	3.67 ± 0.06^{ac}	3.88 ± 0.14^{a}
Val	5.11 ± 0.05^{a}	5.11 ± 0.33^{a}	4.99 ± 0.02^{ab}	4.80 ± 0.15^{b}	4.71 ± 0.00^{bc}	4.72 ± 0.10^{b}
Met	1.05 ± 0.09^{a}	0.75 ± 0.22^{abd}	0.63 ± 0.38^{bd}	0.26 ± 0.06^{bc}	0.41 ± 0.03^{b}	0.57 ± 0.21^{b}
Cys	0.58 ± 0.12^{a}	0.40 ± 0.04^{b}	0.51 ± 0.17^{ab}	0.59 ± 0.06^{a}	0.62 ± 0.01^{a}	0.66 ± 0.11^{a}
Ile	3.49 ± 0.03^{a}	3.58 ± 0.28^{a}	3.46 ± 0.10^{a}	3.17 ± 0.16^{b}	3.14 ± 0.06^{b}	3.06 ± 0.05^{b}
Leu	4.90 ± 0.04^{a}	4.92 ± 0.42^{a}	4.66 ± 0.11^{ab}	4.41 ± 0.18^{b}	4.36 ± 0.08^{b}	4.33 ± 0.11^{b}
Trp	2.11 ± 1.88^{a}	1.40 ± 0.21^{ab}	1.89 ± 1.10^{ab}	1.14 ± 0.08^{ab}	0.48 ± 0.06^{b}	1.24 ± 0.10^{ab}
Phe	2.11 ± 1.23^{a}	2.41 ± 0.34^{a}	2.09 ± 0.32^{a}	2.21 ± 0.11^{a}	2.53 ± 0.15^{a}	1.97 ± 1.26^{a}
His	4.53 ± 0.57^{abd}	5.28 ± 0.30^{ad}	5.40 ± 0.32^{ad}	5.87 ± 0.31^{acd}	5.59 ± 0.26^{abcd}	6.59 ± 1.40^{ac}
Lys	10.71 ± 0.68^{a}	11.13 ± 1.66^{a}	10.36 ± 0.23^{a}	10.16 ± 0.28^{a}	10.65 ± 0.27^{a}	10.79 ± 0.78^{a}
Tyr	9.22 ± 1.64^{a}	8.53 ± 6.42^{a}	6.65 ± 0.17^{a}	8.73 ± 0.15^{a}	9.00 ± 0.12^{a}	5.48 ± 2.59^{a}

Different letters across a row indicate significant difference ($P < 0.05$).

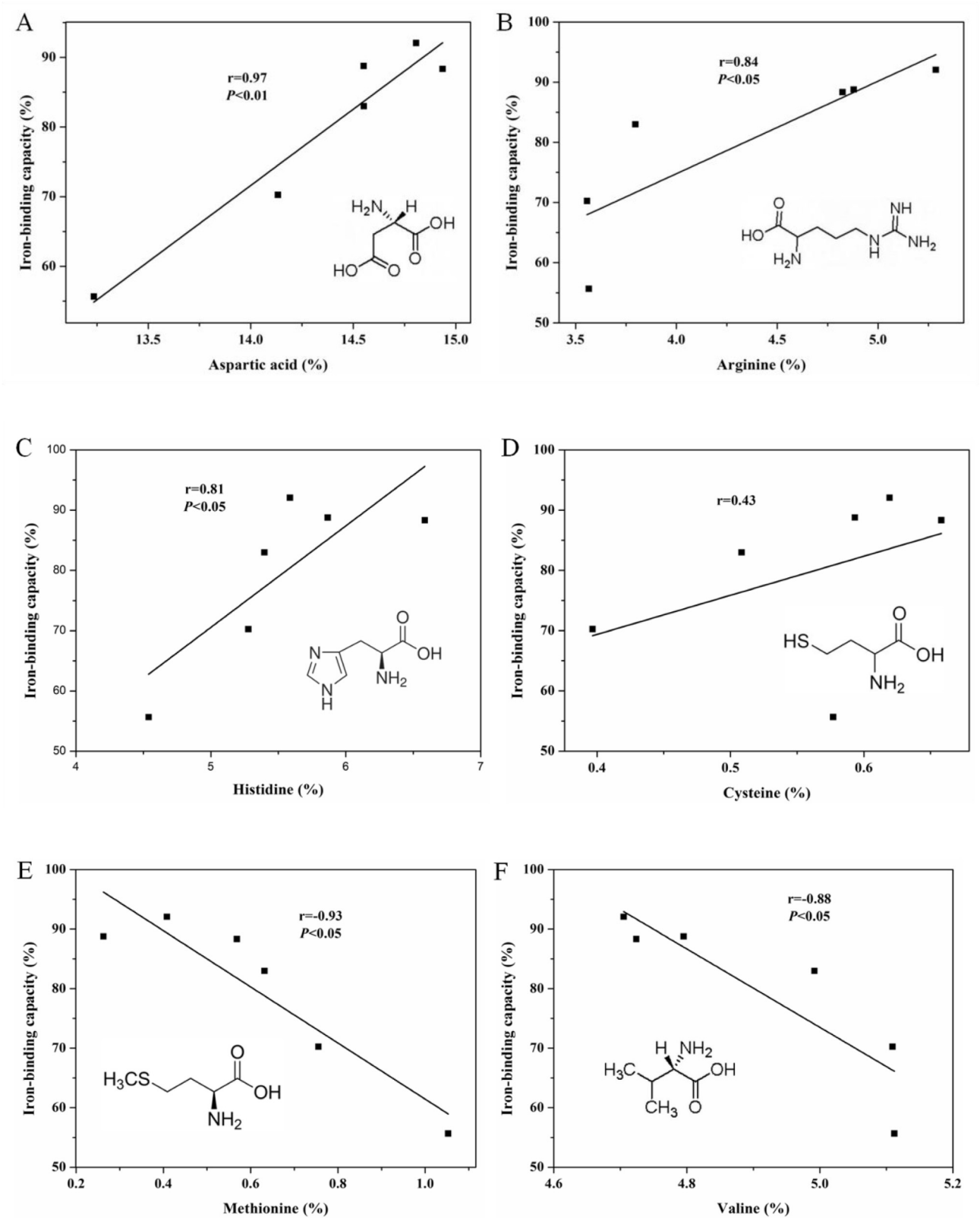

Fig. 3. Correlation of iron-binding activity of the SCOHs with the relative content of their amino acids. (A) Asp; (B) Arg; (C) His; (D) Cys; (E) Met; (F) Val. The Spearman Rank Correlation Coefficient r-value and the associated *P*-value are shown for each panel.

amongst the main iron-binding sites. In our study, a close correlation ($r = 0.97$, $P < 0.01$) was found between Asp content and iron-binding activity, as indicated in Fig. 3A.

Histidine, which has a high binding capacity owing to its N-containing imidazole ring, is directly implicated in peptide binding to metal ions. There was a close correlation ($r = 0.81$) between

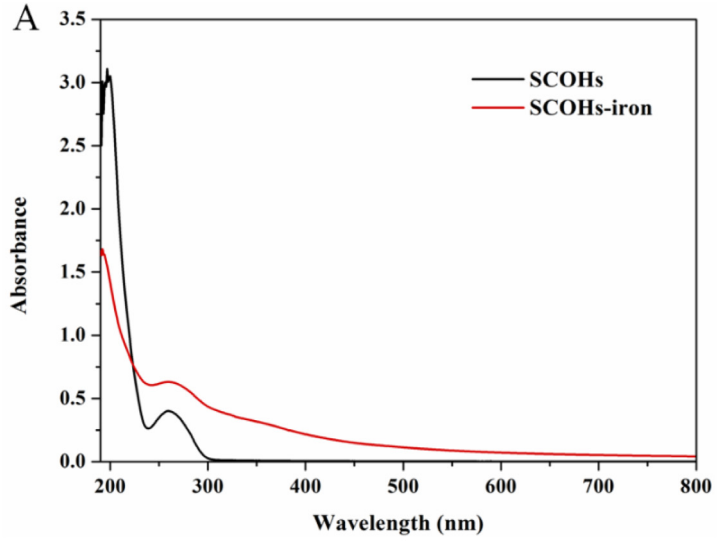

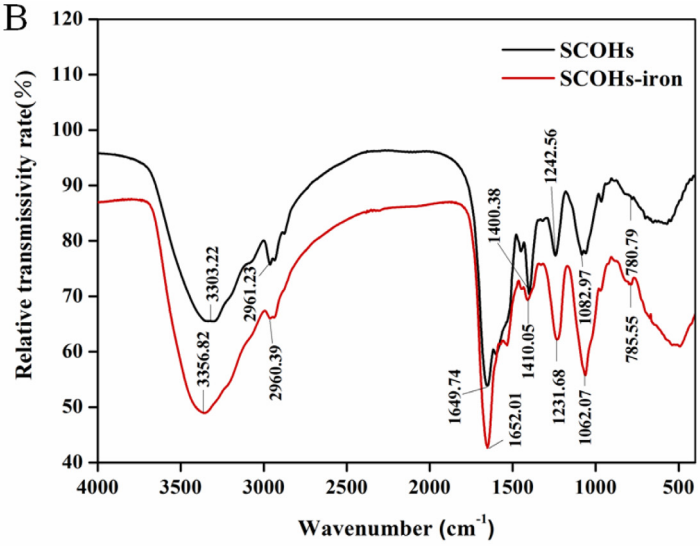

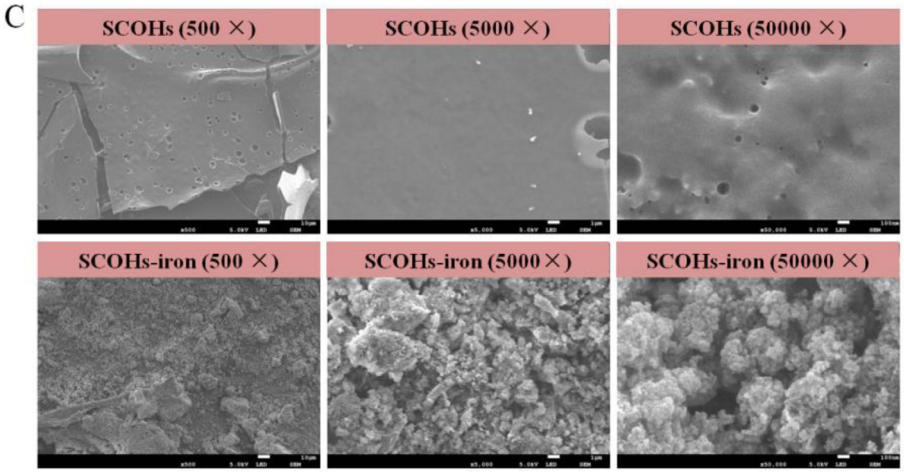

Fig. 4. Structural and physical characterization of the SCOHs and SCOHs-iron complexes. (A) UV–vis spectra of the SCOHs and SCOHs-iron over the wavelength range from 190 to 800 nm. (B) FTIR spectra of the SCOHs and SCOHs-iron in the regions from 4000 to 400 cm^{-1}. (C) Microstructure of the SCOHs and SCOHs-iron complexes determined by scanning electron microscopy. The electron micrographs of the SCOHs and SCOHs-iron complexes at a magnification factor of 500, 5000 and 50000-fold were shown.

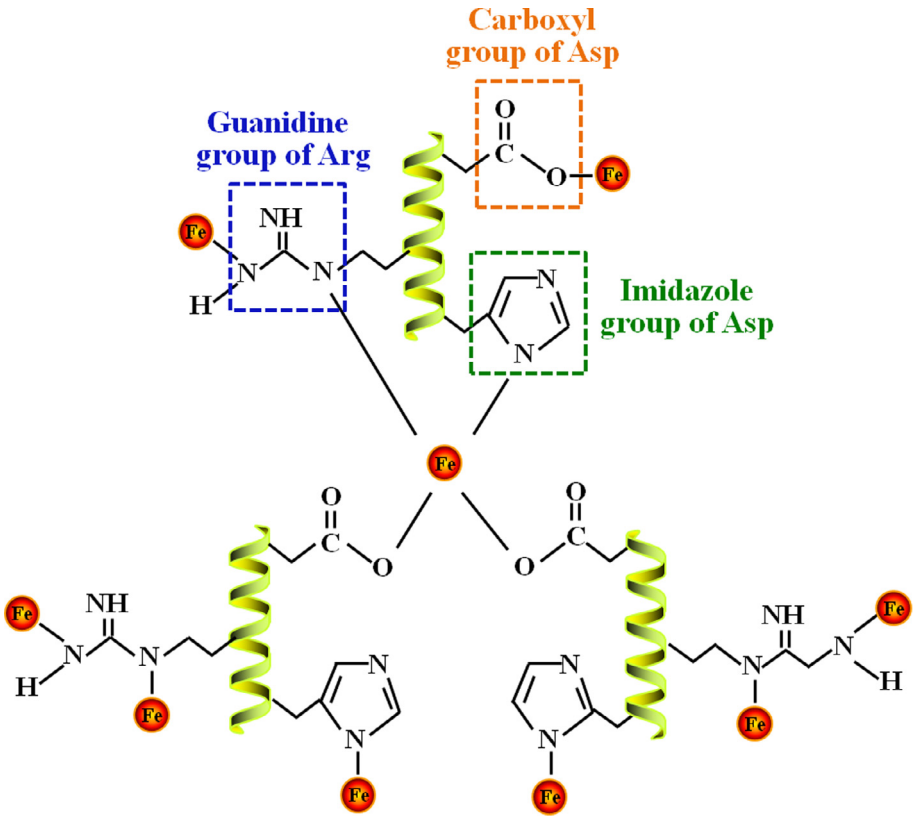

Fig. 5. A simplified model of iron-binding sites on the SCOHs.

the histidine content in the SCOHs and the iron-binding activity (Fig. 3C). Histidine is also essential for the binding of ferric iron to lactoferrin, where the iron-binding active site consists of a histidine, an aspartate residue, and two tyrosines (Nicholson et al., 1997). Moreover, peptides derived from soy protein rich in histidine have been reported to stabilize pro-oxidative transitional metal ions (Amadou, Le, Shi, & Jin, 2011).

Cysteine has been recognized as an important amino acid associated with iron binding, especially when derived from meat protein digestion (Glahn & Van Campen, 1997). However, in this case, no correlation was observed between cysteine content and iron binding (Fig. 3D), which is consistent with chickpea-chelating peptides reported by Torres-Fuentes et al. (2012).

3.6. Structural characterization of SCOHs-iron complexes

3.6.1. Ultraviolet–visible spectra analysis

Ultraviolet–visible (UV–Vis) spectroscopy assay was performed to investigate the formation of SCOHs-iron complexes. The formation of complexes of organic ligands and metal ions induces the shifting or disappearance of pre-existing absorbance peaks or the appearance of new ones. As shown in Fig. 4A, the maximum absorption peak at 197 nm disappeared after the addition of $FeCl_2$ to the SCOHs, which suggests that the nitrogen atom of the amido bond was involved in the formation of the SCOHs-iron complexes (Anderson, Bendell, & Groundwater, 2004; Zhou et al., 2012). Another absorption peak at around 260 nm appeared for both the SCOHs and SCOHs-iron complexes, resulting from the characteristic UV absorption of aromatic amino acids such as tryptophan, tyrosine, and phenylalanine. With the addition of iron ions to the SCOHs, the intensity of the absorption peaks of aromatic amino acids became higher than that of the SCOHs ($P < 0.05$), which may be attributed to relevant valence electron transition during the binding of the SCOHs with iron (Mach & Middaugh, 1994). All of these changes suggest that the SCOHs can bind with iron ions and, therefore, form SCOHs-iron complexes.

3.6.2. FTIR spectroscopy

Changes in the characteristic FTIR absorption peaks of the carboxylates and amides in the SCOHs reflect the interaction of metal ions with organic ligand groups. The FTIR spectra of the SCOHs and SCOHs-iron complexes are shown in Fig. 4B. The absorption band of the SCOHs at 1649.74 cm^{-1} was characterized as an amide I band and attributed to the C=O stretching vibration coupled with the bending vibration of N—H. After binding with iron, the band corresponding to the amide I group moved to a higher wavenumber (1652.01 cm^{-1}), which showed that the C=O group was probably bound to iron ions. Moreover, the absorption at the high wavenumber of 3303.22 cm^{-1} could be attributed to the vibration of N—H (Huang et al., 2011). Because the nitrogen atoms could form coordination bonds with iron ions by offering their electron pairs (van der Ven et al., 2002), the hydrogen bonds were replaced with Fe-N bonds; this was responsible for the shift to higher frequency of 3356.82 from 3303.22 cm^{-1} following iron fortification of the SCOHs. In addition, the SCOHs-iron complexes gave several absorption peaks in the 800–500 cm^{-1} range, which arise from the vibrations of the C—H and N—H bonds in the ion-binding peptide (Chen et al., 2013); these absorption peaks were not present in the spectrum of SCOHs. These data were similar to those for iron-binding peptides from other sources (Huang et al., 2011; O'Loughlin et al., 2015; Zhou et al., 2012), and suggested that the iron-binding sites corresponded primarily to carboxyl oxygen and amino nitrogen atoms.

3.7. Microstructure analysis of SCOHs-iron complexes

The microstructures of the SCOHs and SCOHs-iron complexes were observed using scanning electron microscopy at

magnification factors of 500, 5000, and 50,000, as shown in Fig. 4C. The SCOHs exhibited a smooth amorphous structure consisting of hollows of different sizes. However, the SCOHs-iron complexes showed a fold and crystal structure with spherical particles. The change in the microstructure could be due to the interaction between the SCOHs and the iron ions.

3.8. Simplified model of iron-binding sites on the SCOHs

Based on the results of zeta potential, amino acid composition, and FTIR spectra analysis, we speculate that iron binds to the SCOHs primarily through interactions with the carboxyl oxygen of Asp, guanidine nitrogen of Arg, or nitrogen atoms in the imidazole group of His. A simplified model and schematic diagram (Fig. 5) were established and drawn to interpret the interaction between the SCOHs and the iron ions. The iron ions may be surrounded by these functional binding bonds in the SCOHs through coordination bonds, or form Fe-O and Fe-N bonds with the SCOHs.

4. Conclusion

The dynamic changes in molecular size, surface charge distribution, and exposure of specific amino acids during the hydrolysis process, as well as their contributions to the iron-binding capacities of the peptides, have not been comprehensively examined, even though such information is of particular importance for understanding the interaction between peptides and iron ions. In the present study, we found that as the hydrolysis time increased, the molecular size of the SCOHs decreased, the negative charges (e.g., —COO^-) increased, and the hydrophilic amino acids (e.g., Asp, Arg, and His) were exposed to the surface, facilitating iron binding. Furthermore, a possible iron-binding mode of the SCOHs was proposed in which iron bound to the SCOHs primarily through interactions with the carboxyl oxygen of Asp, guanidine nitrogen of Arg, or nitrogen atoms in the imidazole group of His. The formed SCOHs-iron complexes exhibited a fold and crystal structure with spherical particles. This may aid immensely in the understanding of the nature of iron-binding peptides and associated iron binding mechanisms.

Acknowledgements

This work was financially supported by the National Natural Science Foundation of China (NO. 31601471) and the Fundamental Research Funds of Liaoning Education Department, China (NO. 2016J049).

References

Adamson, N. J., & Reynolds, E. C. (1996). Characterization of casein phosphopeptides prepared using alcalase: Determination of enzyme specificity. *Enzyme and Microbial Technology, 19*(3), 202–207.
Adler-Nissen, J. (1986). *Enzymic hydrolysis of food proteins*. Elsevier Applied Science Publishers.
Amadou, I., Le, G. W., Shi, Y. H., & Jin, S. (2011). Reducing, radical scavenging, and chelation properties of fermented soy protein meal hydrolysate by Lactobacillus plantarum LP6. *International Journal of Food Properties, 14*(3), 654–665.
Anderson, R. J., Bendell, D. J., & Groundwater, P. W. (2004). Organic spectroscopic analysis. *Royal Society of Chemistry* (22).
Anderson, S. C., Flemming, J. M., Watson, R., & Lotze, H. K. (2011). Serial exploitation of global sea cucumber fisheries. *Fish and Fisheries, 12*(3), 317–339.
Caetano-Silva, M. E., Bertoldo-Pacheco, M. T., Paes-Leme, A. F., & Netto, F. M. (2015). Iron-binding peptides from whey protein hydrolysates: Evaluation, isolation and sequencing by LC–MS/MS. *Food Research International, 71*, 132–139.
Camaschella, C. (2015). Iron-deficiency anemia. *New England Journal of Medicine, 372*, 1832–1843.
Carrasco-Castilla, J., Hernández-Álvarez, A. J., Jiménez-Martínez, C., Jacinto-Hernández, C., Alaiz, M., Girón-Calle, J., ... Dávila-Ortiz, G. (2012). Antioxidant and metal chelating activities of peptide fractions from phaseolin and bean protein hydrolysates. *Food Chemistry, 135*(3), 1789–1795.
Chen, D., Liu, Z., Huang, W., Zhao, Y., Dong, S., & Zeng, M. (2013). Purification and characterisation of a zinc-binding peptide from oyster protein hydrolysate. *Journal of Functional Foods, 5*(2), 689–697.
Glahn, R. P., & Van Campen, D. R. (1997). Iron uptake is enhanced in Caco-2 cell monolayers by cysteine and reduced cysteinyl glycine. *The Journal of Nutrition, 127*(4), 642–647.
Huang, G., Ren, Z., & Jiang, J. (2011). Separation of iron-binding peptides from shrimp processing by-products hydrolysates. *Food and Bioprocess Technology, 4*(8), 1527–1532.
Hurrell, R., & Egli, I. (2010). Iron bioavailability and dietary reference values. *The American Journal of Clinical Nutrition, 91*(5), 1461S–1467S.
Jin, Y., Liang, R., Liu, J., Lin, S., Yu, Y., & Cheng, S. (2017). Effect of structure changes on hydrolysis degree, moisture state, and thermal denaturation of egg white protein treated by electron beam irradiation. *LWT-Food Science and Technology, 77*, 134–141.
Kim, S. B., Seo, I. S., Khan, M. A., Ki, K. S., Nam, M. S., & Kim, H. S. (2007). Separation of iron-binding protein from whey through enzymatic hydrolysis. *International Dairy Journal, 17*(6), 625–631.
Lee, S. H., & Song, K. B. (2009). Purification of an iron-binding nona-peptide from hydrolysates of porcine blood plasma protein. *Process Biochemistry, 44*(3), 378–381.
Lin, S., Liang, R., Xue, P., Zhang, S., Liu, Z., & Dong, X. (2017). Antioxidant activity improvement of identified pine nut peptides by pulsed electric field (PEF) and the mechanism exploration. *LWT-Food Science and Technology, 75*, 366–372.
Mach, H., & Middaugh, C. R. (1994). Simultaneous monitoring of the environment of tryptophan, tyrosine, and phenylalanine residues in proteins by near-ultraviolet second-derivative spectroscopy. *Analytical Biochemistry, 222*(2), 323–331.
Martınez-Navarrete, N., Camacho, M. M., Martınez-Lahuerta, J., Martınez-Monzó, J., & Fito, P. (2002). Iron deficiency and iron fortified foods—a review. *Food Research International, 35*(2), 225–231.
McLean, E., Cogswell, M., Egli, I., Wojdyla, D., & De Benoist, B. (2009). Worldwide prevalence of anaemia, WHO vitamin and mineral nutrition information system, 1993–2005. *Public Health Nutrition, 12*(04), 444–454.
Nchienzia, H. A., Morawicki, R. O., & Gadang, V. P. (2010). Enzymatic hydrolysis of poultry meal with endo-and exopeptidases. *Poultry Science, 89*(10), 2273–2280.
Nicholson, H., Anderson, B. F., Bland, T., Shewry, S. C., Tweedie, J. W., & Baker, E. N. (1997). Mutagenesis of the histidine ligand in human lactoferrin: iron binding properties and crystal structure of the histidine-253→ methionine mutant. *Biochemistry, 36*(2), 341–346.
O'Loughlin, I. B., Kelly, P. M., Murray, B. A., FitzGerald, R. J., & Brodkorb, A. (2015). Molecular characterization of whey protein hydrolysate fractions with ferrous chelating and enhanced iron solubility capabilities. *Journal of Agricultural and Food Chemistry, 63*(10), 2708–2714.
Pereira, P. M. D. C. C., & Vicente, A. F. D. R. B. (2013). Meat nutritional composition and nutritive role in the human diet. *Meat Science, 93*(3), 586–592.
Puig, S., Askeland, E., & Thiele, D. J. (2005). Coordinated remodeling of cellular metabolism during iron deficiency through targeted mRNA degradation. *Cell, 120*(1), 99–110.
Seth, A., & Mahoney, R. R. (2000). Binding of iron by chicken muscle protein digests: the size of the iron-binding peptides. *Journal of the Science of Food and Agriculture, 80*(11), 1595–1600.
Smyth, M., & FitzGerald, R. J. (1998). Relationship between some characteristics of WPC hydrolysates and the enzyme complement in commercially available proteinase preparations. *International Dairy Journal, 8*(9), 819–827.
Stevens, G. A., Finucane, M. M., De-Regil, L. M., Paciorek, C. J., Flaxman, S. R., & Branca, F. ... (2013)Global, regional, and national trends in hemoglobin concentration and prevalence of total and severe anaemia in children and pregnant and non-pregnant women for 1995–2011: a systematic analysis of population-representative data, (2013). *The Lancet Global Health, 1*(1), 1625.
Storcksdieck, S., Bonsmann, G., & Hurrell, R. F. (2007). Iron-binding properties, amino acid composition, and structure of muscle tissue peptides from in vitro digestion of different meat sources. *Journal of Food Science, 72*(1), S019–S029.
Sukan, G., & Andrews, A. T. (1982). Application of the plastein reaction to caseins and to skim-milk powder: II. Chemical and physical properties of the plasteins and the mechanism of plastein formation. *Journal of Dairy Research, 49*(02), 279–293.
Sun, N., Wu, H., Du, M., Tang, Y., Liu, H., Fu, Y., & Zhu, B. (2016). Food protein-derived calcium chelating peptides: A review. *Trends in Food Science & Technology, 58*, 140–148.
Torres-Fuentes, C., Alaiz, M., & Vioque, J. (2012). Iron-chelating activity of chickpea protein hydrolysate peptides. *Food Chemistry, 134*(3), 1585–1588.
van der Ven, C., Muresan, S., Gruppen, H., de Bont, D. B., Merck, K. B., & Voragen, A. G. (2002). FTIR spectra of whey and casein hydrolysates in relation to their functional properties. *Journal of Agricultural and Food Chemistry, 50*(24), 6943–6950.
Vanapalli, S., & Coupland, J. N. (2000). Characterization of food colloids by phase analysis light scattering. *Food Hydrocolloids, 14*, 315–317.
Wang, X., Li, M., Li, M., Mao, X., Zhou, J., & Ren, F. (2011). Preparation and characteristics of yak casein hydrolysate–iron complex. *International Journal of Food Science & Technology, 46*(8), 1705–1710.
Wang, L. L., & Xiong, Y. L. (2005). Inhibition of lipid oxidation in cooked beef patties by hydrolyzed potato protein is related to its reducing and radical scavenging ability. *Journal of Agricultural and Food Chemistry, 53*(23), 9186–9192.
Wang, X., Zhou, J., Tong, P. S., & Mao, X. Y. (2011). Zinc-binding capacity of yak casein hydrolysate and the zinc-releasing characteristics of casein hydrolysate-zinc complexes. *Journal of Dairy Science, 94*(6), 2731–2740.

Wu, H. T., Jin, W. G., Sun, S. G., Li, X. S., Duan, X. H., & Li, Y. ... (2016)Identification of antioxidant peptides from protein hydrolysates of scallop (Patinopecten yessoensis) female gonads, (2016). *European Food Research and Technology, 242*(5), 713–722.

Wu, H., Liu, Z., Zhao, Y., & Zeng, M. (2012). Enzymatic preparation and characterization of iron-chelating peptides from anchovy (Engraulis japonicus) muscle protein. *Food Research International, 48*(2), 435–441.

Zhang, M. N., Huang, G. R., & Jiang, J. X. (2014). Iron binding capacity of dephytinised soy protein isolate hydrolysate as influenced by the degree of hydrolysis and enzyme type. *Journal of Food Science and Technology, 51*(5), 994–999.

Zhou, J., Wang, X., Ai, T., Cheng, X., Guo, H. Y., Teng, G. X., & Mao, X. Y. (2012). Preparation and characterization of β-lactoglobulin hydrolysate-iron complexes. *Journal of Dairy Science, 95*(8), 4230–4236.